Reptation of a Polymer Chain in an Irregular Matrix: Diffusion and Electrophoresis

Bruno H. Zimm*

Department of Chemistry, University of California, San Diego, 9500 Gilman Drive, La Jolla, California 92093-0317

Oscar Lumpkin

Department of Physics, University of California, San Diego, 9500 Gilman Drive, La Jolla, California 92093-0319

Received July 21, 1992; Revised Manuscript Received October 5, 1992

ABSTRACT: A simple version of the reptation theory of motion of polymer chains through random matrices is extended by adding a free energy of interaction between the moving chain (the "probe") and the matrix. This free energy is assumed to depend on the position of the probe and to fluctuate randomly as the probe moves. The electrophoretic mobility and diffusion constant of the probe are calculated by numerical integration of the diffusion equation. It is found that the probe sometimes falls into low-free-energy states that act as temporary traps. These traps can dramatically slow the motion of the probe, depending on the values of the interaction free energy and a possible external field, if any. The dependence of the diffusion constant on probe size N changes from the classical reptation N^{-2} at small N to an exponential dependence at large N. The electrophoretic mobility has a more complex behavior that depends on the strength of the electric field. With low fields the mobility shows the classical N^{-1} at small N, is markedly depressed at intermediate N, and becomes classical again at large N. (With sufficiently high fields the behavior is classical at all N.) The depression at intermediate N can make the mobility depend very steeply on size over a short range of sizes and can also produce "band inversion", where larger probes move faster than smaller ones. In the region of the depression the migrating band can be greatly broadened.

1. Introduction

In the reptation theory of the gel electrophoresis of DNA it is most commonly assumed that all spaces in the gel are energetically equivalent to the migrating probe molecules.[1,2] The same concept is used in the reptation theory of diffusion of a polymer chain through a matrix of obstacles, such as other chains.[3,4] But this assumption is probably not true in the case of a stiff chain, such as DNA, as the probe molecule in a tight gel, such as polyacrylamide. When the probe moves into a long, narrow, curved space either the probe must bend or the gel must deform, or both, with an energetic cost.

In a recent paper Calladine and co-workers[5] have presented experimental results on the electrophoresis of DNA in various gels that show a region of remarkably steep decline of mobility with the length of the DNA probes, the mobility frequently approaching a dependence on the −3 power of the length at long lengths. Arvanitidou and Hoagland,[6] working with poly(styrene sulfonate) in polyacrylamide, likewise found dependences as high as the −2.4 power, in this case at intermediate lengths. Such steep dependences are not explained by current theory based on the reptation picture[1,2] with no energetic component. Such theories give a dependence on the inverse first power or less, or even a dependence with a positive exponent ("band inversion") at high fields and chain lengths. (We are not talking here about electrophoresis in pulsed fields; all the cited results refer to a steady electric field.)

It is also well-known that the diffusion of polymer chains in a matrix of obstacles is not completely described by reptation theory, which predicts that the diffusion constant should scale as the inverse second power of the probe length;[3,4] for long probes the dependence on length is usually steeper than this. (This is a large literature on diffusion of chains in a matrix; see, for example, refs 7–11.) Baumgärtner and Muthukumar[12] have shown that the steepening can be produced by a random array of obstacles making entropic barriers along the diffusion path; see also Muthukumar and Baumgärtner[13] and Honeycutt and Thirumalai.[14]

Thus there is reason to consider a reptation model in which a variable position-dependent free energy is explicitly included. Such a free energy sometimes randomly drops to an unusually low value, effectively creating a trap. In this paper we introduce a simple model of this type, not attempting to provide a detailed molecular picture but merely assuming that the free energy is a random variable. Even from such a general model interesting results appear, reminiscent of the diffusion data and of the electrophoretic data of Calladine et al.[5] We find, for example, that a steep dependence of electrophoretic mobility on chain length, frequently reaching or even exceeding the third power, is easily obtained, sometimes accompanied by the opposite effect, band inversion. Another result is extreme broadening of the profile of the migrating band under some circumstances. The dependence of the diffusion coefficient on size can change from power law to exponential. Thus inclusion of energetics in the theory leads to the appearance of a new set of interesting phenomena.

2. Model

Our strategy is to deal first with the electrophoresis problem, computing the mobility of the probe under the influence of a steady force. From the low-field limit of this mobility we can then get the diffusion constant. We use the familiar tight-tube reptation model,[2] in effect assuming that the probe is much longer than the interfiber spacing. The probe, modeled as a chain of N rigid segments ("Kuhn lengths") joined by universal joints, is assumed to be confined tightly to a (possibly biased) random-walk tube, the probe not being allowed to bend away from the tube axis. This tube is supposed to be embedded in a matrix, the "gel", of very sluggish or actually cross-linked chains, so that the probe can move only along the axis of the tube. The curvilinear axial coordinate in the tube is

0024-9297/93/2226-0226$04.00/0

s. The electric field is parallel to the Cartesian coordinate, x. The segments of the probe interact with the surrounding matrix with a free energy that fluctuates with the s-coordinate of the segment as the segment moves along s. This picture depends on the assumption that the matrix has a structure that remains fixed over the time that the probe segment occupies one position, which is probably appropriate for a cross-linked gel but is questionable if the matrix consists only of free though slowly moving chains. In the latter case the lifetime of conformations of the matrix would come into play; we do not deal with this problem in this paper. In the case of a fixed matrix the probe has a definite total free energy at any position, the sum of the free energies of its constituent segments.

This model differs from the more general reptation model of de Gennes and of Doi and Edwards in that there is no tube-renewal process; we consider an ensemble of systems, but in one system of the ensemble the probe moves backward and forward in one, unchanging tube. The tube is changed only when we go to a new member of the ensemble of systems. The results reported here are averages over this ensemble.

Since its parts fluctuate as the probe moves, the total free energy of the probe is a random variable, and on occasion its gradient may become too steep for the electric field alone to pull the probe to the next position, thus creating a free-energy trap. We then have to include Brownian motion in the model to help the probe escape. We do this by explicitly including a diffusion term and using Fick's law. When deep traps are present, this procedure seems to be computationally more efficient than simply generating a series of chains, adding Brownian motion, and averaging the electrophoretic velocities.

3. Methods

We consider an ensemble of identical systems in the steady state, with $C_s(s)$ the concentration in the ensemble of a reference point of each of the probes; C_s is a function of position, s, along the tube. (The reference point can be any defined point in the probe, such as the central segment.) This C_s is assumed to obey the one-dimensional diffusion equation with an external-force term:

$$\frac{dC_s}{dt} = -\frac{dJ}{ds} = D\frac{d}{ds}\left(\frac{dC_s}{ds} + \frac{C_s}{k_bT}\frac{d\Phi}{ds}\right) \tag{1}$$

Here J is the current of systems flowing along s, D is the diffusion coefficient, k_b and T are Boltzmann's constant and temperature, and Φ, a function of s, is the free energy of the probe chain. The free-energy function, $\Phi(s)$, contains not only the usual energy from the external electric field but also a term from the interaction of the probe chain with the gel; this is the term that sometimes creates traps.

We consider the ensemble to be in the steady state, with an infinite number of systems distributed along the path as described by $C_s(s)$. Because of the steady state, $dC_s/dt = -dJ/ds$ is zero everywhere, so J is constant and eq 1 can be integrated once, giving us only a first-order differential equation to solve:

$$J = -D\left(\frac{dC_s}{ds} + \frac{C_s}{k_bT}\frac{d\Phi}{ds}\right) \tag{2}$$

Projection from s to x. We need to convert from the tube coordinate, s, to the laboratory coordinate, x, along which the external electric field is directed. We need to define a reference point for the probe in x, and we take this to be the x-coordinate of its center of mass. We then convert dC_s/ds to

$$\frac{dC_s}{ds} = \frac{dx}{ds}\frac{dC_s}{dx} \tag{3}$$

In converting from s to x, we require that the number of systems $C_s\,ds$ in a section, ds, of path be the same regardless of which coordinate is used, which requires that C_x, the concentration in terms of x, obey the relation

$$C_s\,ds = C_x\,dx \tag{4}$$

which gives

$$C_s = \frac{dx}{ds}C_x \tag{5}$$

Then the first term of eq 2 expressed in terms of C_x is

$$-D\left(\frac{dx}{ds}\right)^2\frac{dC_x}{dx} \tag{6}$$

We can do a similar projection with the second term in J; we convert the motion along s to motion along x with one factor of dx/ds and convert the derivative with respect to s to a derivative with respect to x with a second identical factor. (Actually, this discussion is incomplete because it is possible for s to be a many-valued function of x if the tube is sufficiently convoluted. In that case we sum over the C_s terms corresponding to the different sections of tube having the same x in eqs 3–5.)

To evaluate dx/ds, we follow previous work.[2] Consider the probe to be made up of segments each of length Δs_i, mass m_i, located at x_i, and making an angle θ_i with the x-axis. The total mass of the probe is M. Then the velocity of the center of mass is by definition

$$\dot{x} = (1/M)\sum m_i\dot{x}_i \tag{7}$$

From the assumption of motion strictly along the tube axis we get

$$\dot{x}_i = \dot{s}\cos\theta_i \tag{8}$$

Further, with L the total length of the probe the mass of a segment is

$$m_i = (M/L)\Delta s_i \tag{9}$$

Putting the last three equations together gives

$$\dot{x} = (h_x/L)\dot{s} \tag{10}$$

where h_x is the x-component of the end-to-end distance:

$$h_x = \sum \Delta s_i\cos\theta_i \tag{11}$$

From this follows

$$dx/ds = h_x/L \tag{12}$$

The result of carrying out these projections is

$$J = -PD\left(\frac{dC_x}{dx} + C_x\frac{d\Psi}{dx}\right) \tag{13}$$

where

$$P = \left(\frac{dx}{ds}\right)^2 = \left(\frac{h_x}{L}\right)^2 \tag{14}$$

is the projection factor, and

$$\Psi = \Phi/k_bT \tag{15}$$

is the free energy in units of k_bT.

Since J is constant, eq 13 is a differential equation for C_x as a function of the reduced free energy, Ψ, and the projection factor, P. We can simplify further by defining

a reduced concentration, W, as

$$W = DC_x/J \tag{16}$$

and eq 13 can be put into conventional form as

$$\frac{dW}{dx} + W\frac{d\Psi}{dx} = -\frac{1}{P} \tag{17}$$

Velocity. The average of the x-component of the probe velocity is defined as

$$\langle \dot{x} \rangle = \frac{x}{t} = \int_0^x dx' / \int_0^t dt' \tag{18}$$

where x is the total distance traveled and t is the total time, and the prime indicates a variable being integrated. The current, J, at any point is the x-component of the velocity of the probes at that point, $\dot{x}$, times the concentration, C_x, at that point. Therefore, $dt' = dx'/\dot{x} = C_x dx'/J$. Combining these relations and remembering that J is constant, we get

$$\langle \dot{x} \rangle = \frac{xJ}{\int_0^x C_x(x')\,dx'} = \frac{xD}{\int_0^x W(x')\,dx'} \tag{19}$$

As a reference we propose to use the velocity of a probe molecule perfectly aligned with the field and with no local fluctuating free energies. If the field is E, the charge of a segment is q, and the friction coefficient of a segment is ζ, so that $N\zeta = k_bT/D$, then this reference velocity is

$$\langle \dot{x}_0 \rangle = qE/\zeta = DNqE/k_bT \tag{20}$$

Combining eqs 19 and 20, we get

$$\frac{\langle \dot{x} \rangle}{\langle \dot{x}_0 \rangle} = \frac{x}{(NqE/k_bT)\int_0^x W(x')\,dx'} \tag{21}$$

We see that the average velocity is determined by the average concentration in the system. The higher this average concentration, the slower the probes are moving.

Integration. To get the concentration, we must integrate eq 17 with an appropriate potential function and with an appropriate P. In accordance with our starting assumptions, we take the potential, Ψ, to be the sum of a term from the field plus a fluctuating term, G, arising from local interactions between the probe and the gel:

$$\Psi = (-NqEx + G)/k_bT \tag{22}$$

The equation can be integrated numerically by standard methods, but we must be careful; if the integration starts from an arbitrary initial condition and progresses in the positive x-direction with E positive, the integration is unstable, W soon diverging toward positive or negative infinity. This problem is solved by integrating backward in the negative x-direction from an arbitrary final condition; then the integration is stable, and the effect of the initial conditions declines exponentially with x. In other words, we select a state at $x = 0$ and integrate backward along x to see what states at negative x-values must have led to it.

The integration can be speeded up by noting that neither Ψ nor P is expected to vary much over a distance δx, such that $|\delta x| \leq |h_x|$; if we approximate these as constants over this interval, we can integrate eq 17 analytically over the interval. The complete integration can then be done in a series of steps, each over an interval δx. In most of the work that follows we make δx equal to $-|h_x|$; this rather large value of δx sacrifices some unneeded accuracy to gain speed and convenience. Taking W_i as the value of W at the beginning of the interval and defining a reduced force, F

$$F = -d\Psi/dx \tag{23}$$

by integrating eq 17 we get at the end of the interval

$$W = \left(W_i - \frac{1}{FP}\right)\exp(F\,\delta x) + \frac{1}{FP} \tag{24}$$

and

$$\int_0^{\delta x} W(x)\,dx = \frac{\delta x}{FP} + \frac{1/FP - W_i}{F}[1 - \exp(F\,\delta x)] \tag{25}$$

We remind ourselves that δx must be negative for stability when E, and hence the average F, is positive. Equation 24 then shows that W tends to drift toward a constant, an "attractor", $1/FP$, whatever its starting value. If we substitute this attractor for W in eq 21, using NqE/k_bT for F, we find that

$$\dot{x}_{attr} = P\langle \dot{x}_0 \rangle \tag{26}$$

In other words, the velocity due to the attractor alone is just the velocity to be expected from the field, after taking account of the projections from the x-coordinate to the s-coordinate and back again. This $\langle \dot{x}_{attr} \rangle$ is used below in estimating the average lifetime of a step across the interval δx.

To integrate now over a long path from 0 to some large negative value, $-x$, we generate a series of steps, $\delta x < 0$, making the final W of the each step the initial W_i of the following step. To get the average velocity, we simply sum the integrals of W from each step, eq 25, and put the result in eq 21. The value of W used to start the whole sequence at $x = 0$ is found from a preliminary run that starts with W equal to the attractor, $1/FP$, with P equal to unity, corresponding to probe perfectly aligned with the field, and with F given by the electric term alone, $F_e = NqE/k_bT$. By eq 17 this forces dW/dx to be zero at $x = 0$, thereby fixing the one arbitrary constant of the solution of the first-order differential equation. In order to allow the initial bias to die out, we then run over a distance $2/F_e$ but using the complete F in each step. The final W of this run is used to start the main integration.

Projection Factor. In generating the steps we must create values for the projection factor, P, and the force, F. We use a very simple model for which most of the work has already been published.[15] The probe is assumed to be a chain having N segments of unit length which are oriented along the x-direction, either upfield or downfield. The probabilities of the two orientations are determined by Boltzmann factors, d for down and u for up:

$$d = \frac{e^{E'}}{e^{E'} + e^{-E'}} \tag{27a}$$

$$u = \frac{e^{-E'}}{e^{E'} + e^{-E'}} \tag{27b}$$

The dimensionless energy $E' = qaE/2k_bT$, where q, a, and E are respectively the charge on the probe segment, the length of a gel pore, and the applied electric field, is a common parameter in reptation models of polyelectrolytes.[16-18] The probe makes random moves of unit length forward and backward by diffusion biased by the field, the downfield move being favored by another Boltzmann factor, $e^{-2\delta}$, where $\delta = |h_x|E'$. The probabilities of various values of h_x are then determined by a set of master differential-difference equations, eqs 5 of ref 15, which are easily solved for the steady-state, time-independent case needed in this work. We require that only

odd values h_x are allowed in order to avoid the singular situation of vanishing h_x (values of h_x must be all odd or all even, since only transitions of 2 units, corresponding to the reversal of a segment, are allowed in this model.) The result is a table of probabilities, $p(h_x)$, for values of h_x. When the a or E' are small, these probabilities are just the binomial distribution corresponding to the number of ways the probe can be folded to obtain a given h_x.

In using this table, we must remember that the probability of occurrence of steps with a particular value of h_x is the product of $r(h_x)$, the frequency of selection of that value at the beginning of the step, with the lifetime, τ, of the step:

$$p(h_x) = r(h_x)\,\tau \tag{28}$$

We estimate τ using the approximate velocity due to the external field alone, $\dot{x}_{attr}$, from eq 26; $\tau = |h_x|/\dot{x}_{attr}$. Substituting this into eq 28 and using eq 14, we get

$$r(h_x) = K_r|h_x|p(h_x) \tag{29}$$

where K_r is a constant to be determined by normalization to unity of the sum of $r(h_x)$ over all h_x. We now can create a table of the frequencies, $r(h_x)$. At the beginning of each step a value of h_x is selected randomly with a frequency determined by this table, and the projection factor, P, is computed by eq 14.

Local Free Energy. The force, F, as the derivative of eq 22, contains two terms, one from the external field and one from the local free energy, G. We assume that G is the sum over all segments of free energies, g_i, arsing from the interaction of each segment, i, with the gel. (These free energies, like the total free energy, Ψ, are expressed in units of k_bT.) Here we make an ad hoc model. We assume that the g_i have a distribution, $w_g(g_i)$, with a mean value of m, and a standard deviation of g; m and g will be adjustable parameters.

$$m = \int g_i w_g(g_i)\,dg_i \tag{30a}$$

$$g^2 = \int (g_i - m)^2 w_g(g_i)\,dg_i \tag{30b}$$

We further assume that the correlation length of the matrix is shorter than the segment length of the probe so that there is no correlation between the g_i of one segment and that of its neighbors, $g_{i\pm1}$. We now need the distribution of probabilities of the free energy of the whole chain, G, the sum of all the individual g_i. If the number of segments, N, is large, we can get this from eq 30 by the central limit theorem as a Gaussian function

$$w(G) = \frac{1}{(2\pi N)^{1/2} g} \exp\left[-\frac{(G - Nm)^2}{2Ng^2}\right] \tag{31}$$

with a mean of Nm and a standard deviation of $N^{1/2}g$. (If N is small, less than 10, values of G are better obtained by randomly selecting N values of g from some distribution compatible with eq 30 and adding them up. Since eq 31 approaches the Gaussian in any case by the central limit theorem, the exact form of the distribution function assumed for w_g is not critical. In this work we used $w_g(g_i) = \exp(-g_i/g)/g$, $g_i \geq 0$, which satisfies eq 30a,b.)

The local free-energy contribution to the force F is assumed to be the difference between the G values of two successive conformations of the probe divided by the distance, δx, between their centers of mass. We thus get, adding the term from the electric field

$$F = \frac{G_1 - G_2}{\delta x} + NF_e \tag{32}$$

where G_1 and G_2 are the G values of the two conformations, and F_e is the electric term. It is convenient to express all lengths, such as δx, as dimensionless multiples of the Kuhn segment length, b. When this is done, F becomes dimensionless, and F_e becomes

$$F_e = bqE/k_bT \tag{33}$$

likewise dimensionless.

The calculation of the $p(h_x)$ for the model of ref 15 depends on a set of probabilities for transitions between states of different h_x. These transition probabilities are affected by the difference between the free energy associated with segment i and that associated with segment $i = 1$, so they should now be averaged over this difference. Unfortunately, this does not seem to be a trivial calculation. Since g_i is not correlated with h_x, we postulate that the averaging should not seriously change most of the $p(h_x)$, and we have omitted it in this work.

Summary of Velocity Calculation. Thus in summary our procedure is as follows. The four parameters that characterize a particular system in our model are as follows: N, the total number of segments in the probe; g, the standard deviation of the segment free energies, g_i; a, the length of the pores of the matrix; F_e, the reduced external electric field, eq 33. Notice that m disappears because by eq 30a it only sets the zero of the free-energy scale, and this cancels in eq 32. We express g in units of k_bT. We use a as a parameter to turn orientation on or off at will in order to see its distinctive effects; in terms of segment lengths, a can take values from 0 to 1; with 0 the orientation is turned off. If we consider specifically the case of double-stranded DNA, for consistency with previous work[19] we set the Kuhn segment length, b, to 115 nm and q to 165 electrons and find that F_e is 0.075 times the field, E, in V/cm. Since E is usually not more than about 50 V/cm in practice, F_e should typically be less than 5. With the values of the parameters selected, we first prepare an initial value of the reduced concentration, W, by starting at $x = 0$ and $W_i = 1/F_eP$, and using eq 24 we perform a series of backward steps of magnitudes $\delta x = -h_x$ selected from the frequency distribution, eq 29. This series of steps is continued until x reaches $-2/F_e$; this series attenuates any initial bias. With the resulting W as the new initial W_i, we then restart at $x = 0$ and continue stepping until x passes a preset value, usually −100 000, representing a distance in laboratory units of 1.15 cm. The mobility relative to that of a fully extended probe without trapping ($g = 0$) is then calculated from eq 21. This calculation is repeated a number of times with different sequences of pseudo-random numbers to create the ensemble average of the mobility and to observe the statistics of the variation in the ensemble of independently calculated values.

Remarks. To avoid misconceptions, we emphasize that our method is not a simulation; it is an integration, partly analytical and partly numerical, of the diffusion equation. We integrate the equation in steps of δx which are selected to be short enough so that the parameters do not change greatly during the step, thus allowing approximate analytical integration over the step. The steps are then summed numerically. Steps can be made shorter without changing the results significantly, but the procedure becomes more complicated because h_x is then correlated from one step to the next. These steps have nothing to do with elementary Brownian motions or with the pore

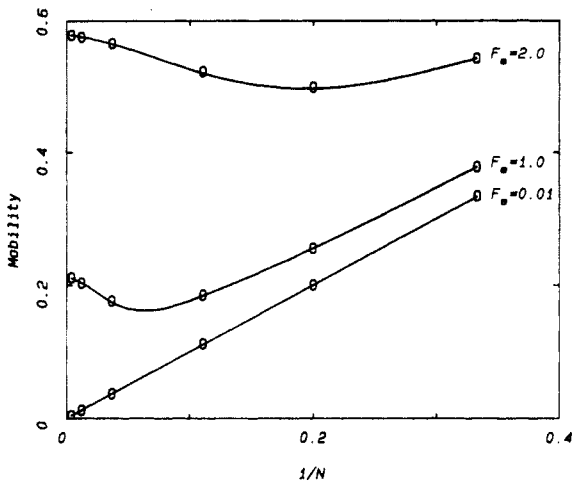

Figure 1. Electrophoretic mobility against $1/N$ for $a = 1$ and $g = 0$. Curves indicate h_x^2/L^2 calculated by the method of ref 15 with cubic-spline interpolation; points indicate the mobility calculated by the method of this paper.

size, a, of the matrix. The latter affects only the tendency of the chain to be oriented by the field, which is expressed in the probability distribution $p(h_x)$.

The average velocity, eq 18, is subject to fluctuations resulting from the random variations of G and P along the path. These fluctuations diminish in proportion to the square root of the path length, $|x|^{-1/2}$, and are insignificant for most of the data points shown, with certain important exceptions discussed below under "broad bands".

4. Results: Electrophoresis

Agreement with the Tight-Tube Reptation Model. We first need to verify that our methods when used on systems without trapping, $g = 0$, give the same results as conventional methods. The test is shown in Figure 1, where mobilities are plotted against the reciprocal of the number of segments, both the new results (points) and the ones published previously[15] (upper two curves); the latter were derived from the same tight-tube reptation model with the mobility defined equal to $\langle h_x^2\rangle/L^2$, which was calculated analytically. (In comparison with the previous publication, note that $E' = F_e/2$ in this case where $a = 1$.) The new results are each the average of a number of runs from $x = 0$ to $x = -100\,000$ with different pseudo-random numbers. The agreement is within the precision of averages. When the field is low (lowest curve), the mobility is strictly proportional to the reciprocal of N, as expected from elementary reptation theory.[1,2] Thus the methods seem to work correctly.

To justify the above comparison, we need to verify that with no traps $\langle h_x^2\rangle/L^2$ is actually the mobility relative to the completely oriented chain, an equality that was simply assumed in ref 15. Let t be the total time for the probe to migrate a distance x. The fraction of this time during which the probe is in a state characterized by a particular value of the projection factor $P_{hx} = h_x^2/L^2$ is $p(h_x)\,t$. The relative velocity $\dot{x}/\dot{x}_0$ while in this state is[2] just P_{hx}. The relative distance moved while in this state is then $p(h_x)\,tP_{hx}$. The relative velocity is the total distance over the total time; this is $\sum p(h_x)\,P_{hx} = \langle P_{hx}\rangle$, which is what was assumed in ref 15.

Effect of Local Free Energy. Now we investigate the effect of including the local free energy. In Figure 2 are log–log plots for the case where the standard deviation of the segmental energy, g, is set to $0.5\,k_bT$, and orientation effects have been turned off by setting a to zero. The top, dashed, curve in the figure is the simple reciprocal relation, mobility proportional to $1/N$, and the points are the

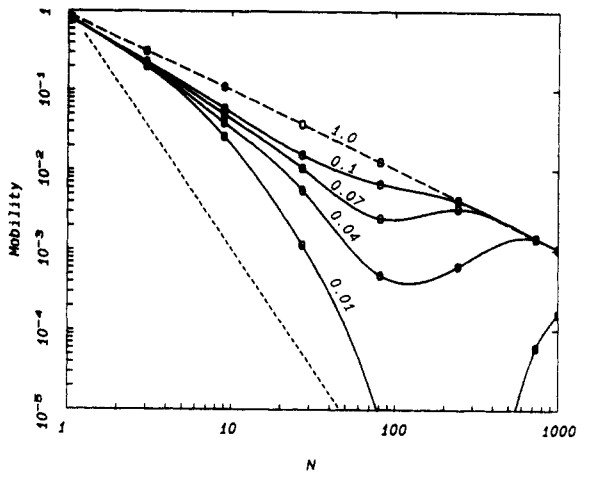

Figure 2. log–log plots of mobility against N for $a = 0$ and $g = 0.5$. The points are calculated values; the curves are cubic-spline interpolation. Some points of the 0.01 calculation are outside the visible plotting area. The numbers on the curves are F_e. The dashed lines have slopes of −1 and −3; the top dashed line also fits the points for $F_e = 1$.

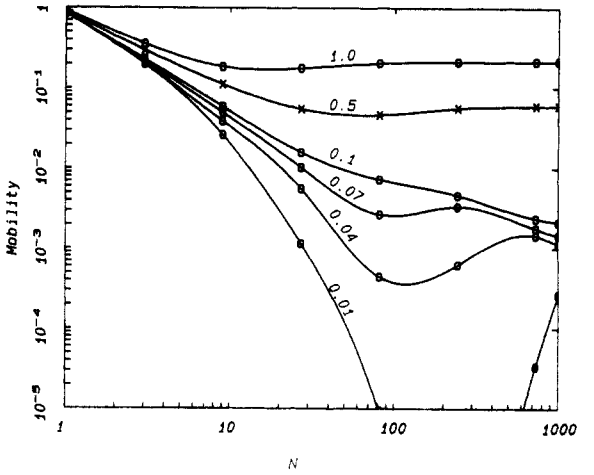

Figure 3. log–log plots of mobility against N for $a = 1$ and $g = 0.5$. The numbers on the curves are F_e.

calculated mobility values for $F_e = 1.0$, which clearly fall on the line. Thus the local free energy has no effect if the field is high enough. But at low fields the effect of g is to reduce the mobility at intermediate values of N; see the lower curves in Figure 2. The reduction at intermediate values of N can be very large, more than a factor of 1000, though the effect disappears at extreme values of N.

Figure 3 shows similar mobility-reducing effects even when the orientation has been turned on by setting a to unity. The orientation effects raise the mobility at high fields and probe lengths, but at low fields the reducing effects of g still predominate.

The mobility reduction is the result of the occurrence along the migration path of occasional places of very slow motion, as shown by the high concentration, W, at these places. The point is illustrated in Table I, where the relative concentration, W, is tabulated as a function of position, x, for a short section of the migration path from three runs on an 81-segment probe with different values of g and F_e. (We recall that W is not the literal physical concentration; it is proportional to the fraction of systems in the ensemble having a particular value of x.) Consider for the moment the two runs with the same external field $F_e = 0.04$, the first with both m and g set to zero and the second with m and g set to 0.5. Both runs used the same set of pseudo-random numbers, so they have the same succession of steps δx, leading to the same values of x (column 1) and the same values of the eq 14 projection

Table I
Profiles of the Projection Factor P, the Force F, and the Relative Concentration W along a Short Section of the x-Axis for Three Runs with $N = 81$ and $a = 0$

		$g = 0, F_e = 0.04$		$g = 0.5, F_e = 0.04$			$g = 0.5, F_e = 1.0$		
x	P	F	W	G	F	W	G	F	W
0	1	3.2	0.31	45.0	3.2	0.31	45.0	81	0.12
−11	0.0184	3.2	16.7	45.0	3.7	14.9	45.0	81.4	0.7
−12	0.0002	3.2	1946.3	33.8	−8.0	2480540	33.8	69.8	94.0
−25	0.0258	3.2	12.0	42.5	3.9	9.9	42.5	81.7	0.5
−32	0.0075	3.2	41.3	34.0	2.0	66.1	34.0	79.8	1.7
−45	0.0258	3.2	12.0	38.4	3.6	10.9	38.4	81.3	0.5
−58	0.0258	3.2	12.0	48.8	4.0	9.6	48.8	81.8	0.5
−73	0.0343	3.2	9.0	41.6	2.8	10.6	41.6	80.5	0.4
−84	0.0184	3.2	16.7	35.5	2.7	20.2	35.5	80.4	0.7
−87	0.0014	3.2	225.0	36.7	3.6	200.4	36.7	81.4	9.0
−104	0.0440	3.2	7.0	36.8	3.2	7.0	36.8	81.0	0.3
−109	0.0038	3.2	81.0	36.8	3.2	81.0	36.8	81.0	3.2
−120	0.0184	3.2	16.7	29.9	2.6	20.8	29.9	80.4	0.7
−131	0.0184	3.2	16.7	35.4	3.7	14.5	35.4	81.5	0.7
−140	0.0123	3.2	25.0	45.1	4.3	18.8	45.1	82.1	1.0

factor P (column 2). It follows from eq 31 that the values of G for the first run are all zero; in column 5 are the G's of the second run. The forces from eq 32 are in columns 3 and 6, and the resulting W's are in columns 4 and 7. (Note that the direction of the current in the ensemble is from the bottom to the top of Table I.) Consider the third line (−12 in the x column); the projection factor is very small because δx is only 1, with the result that systems accumulate at this point, and W becomes large in both columns 4 and 7. But it is seen in column 5 that the free energy is also (accidentally) low at this point, making the force F negative, so the accumulation of W is much larger in column 7 than in column 4. In effect, this location is a trap that systems fall into and out of which they escape very slowly by diffusion. Though the trap is present in both runs because of the low value of P, it is deepened in column 7 because the free energy accidentally happens to be low at this point also, and the effect of free energy on W is exponential by eq 24. Consider now the line beginning with −87 in the x column. This point is also a trap because of the low value of P, but the trap is somewhat counteracted by a higher free energy in column 5, so the accumulation in column 7 is actually less than that in column 4. Since the mobility, $\langle \dot{x} \rangle$, is computed from the sum of all the W's of a given run, the presence of even one deep free-energy trap, like that on the third line, can have an extravagantly large effect on the mobility.

There are at least two kinds of traps, geometric traps and free-energy traps. The third line of Table I illustrates both kinds; in column 4 is a pure geometric trap produced solely by the low value of the projection factor, P, while in column 7 the geometric trap is greatly deepened by the low value of the free energy. In the $x = -87$ line the trap is practically purely geometric in both cases. Geometric traps are already well-known; they are implicitly taken account of in electrophoresis in weak fields by the h_x factor in simple reptation theory.[2] Their exaggerated effect on electrophoresis at higher fields was discovered by Slater and Noolandi and collaborators.[20-23] (Other kinds of traps almost certainly exist, such as blind alleys and molecular lobster pots, but we do not deal with them in this paper.)

The third run, in the last three columns of Table I, shows how a strong external field can overcome a free-energy trap. The value of g is the same as that in the preceding three columns, but now the field is 25 times stronger. The trap is still present at the third line, but its value of W is only about 200 times the value on the next line, in contrast to the 200 000-fold multiplier seen in the preceding case. The force (next-to-last column) stays positive, and the field is effective in helping the systems escape from the trap. The overall effect of g on the mobility is negligible in this case, as shown in the $F_e = 1$ curve in Figure 2.

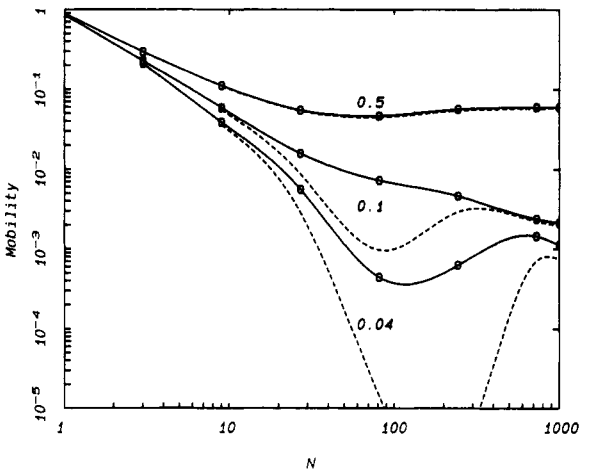

Figure 4. log–log plots of the mobilities of the high-mobility half and the low-mobility half of the migrating band against N for $a = 1$ and $g = 0.5$. From the top down, $F_e = 0.5$, 0.1, and 0.04. Solid curves (from Figure 3) are high mobility; dashed curves are low mobility.

Deep Traps Give Broad Bands. Since deep free-energy traps are rare, they increase the dispersion of mobilities from run to run as well as decrease the value of the mobility averaged over many runs. In experimental terms, they broaden the migrating band. To examine this effect, we have made a group of runs to $x = -100\,000$ and computed two average mobilities, one for the faster migrating half on the group and one for the slower half. Figure 4 shows a few results with parameters the same as those in Figure 3. The solid curves are the averages of the faster migrating half and the dashed curves those of the slower half. The two curves diverge strikingly in the region where the mobility reduction is prominent; in other words, the migrating bands become extremely broad. This is shown more graphically in Figure 5, where we display the band profile as a histogram of mobilities for three cases from Figure 4. When trapping is strong the bands can even become bimodal, as in the middle histogram of Figure 5, with much of the sample never moving perceptibly away from the starting point. (In such cases the average velocity loses most of its significance. We assume that an experimenter would take the forward part of the profile as the band of interest and report a mobility corresponding approximately to our average of the faster half. For this reason we have plotted only the faster halves in Figures 2 and 3.) Of course, if we run the system far enough, the

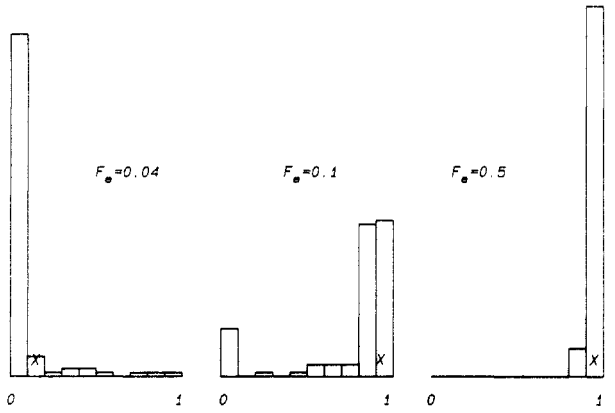

Figure 5. Histograms showing the band profile of some of the points of Figure 4. The abscissa is the mobility; the ordinate is the fraction of the sample. N = 243; a = 1; g = 0.5; F_e = 0.04 (left), 0.1 (middle), 0.5 (right). X marks the average mobility of the faster half of the band.

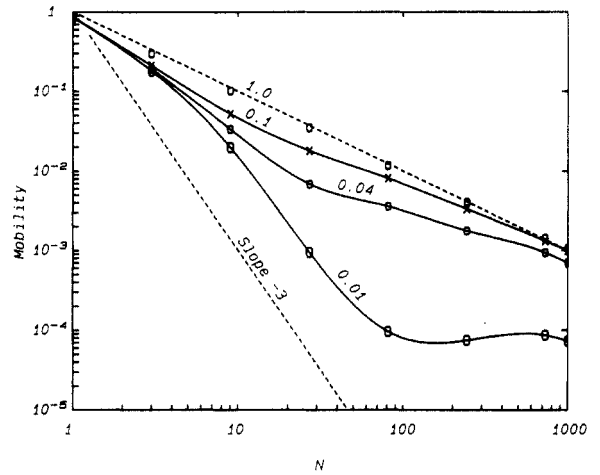

Figure 6. Results of calculation with short steps, as described in the text. Conditions otherwise the same as in Figure 2.

mobility distribution must eventually acquire a Gaussian profile, but with the parameters of the middle pattern of Figure 5 we have not been able to reach this state even at $x = -10^8$, corresponding to a laboratory gel 11 m long; mobilities were still spread over more than a decade.

Short Steps. After the above work was completed, and in response to a reviewer's comment, we made brief study of the effect of reducing the step size, δx. Still with the same model, we generated δx and G by the primitive process of moving the probe instead of taking values from precomputed tables. In each step we advanced the chain in its tube by one segment at a time, adding a new randomly oriented segment at the head and deleting the tail segment. Then the δx of the step was the amount of center of mass moved in the step. A value of $\pm g$, with the sign randomly chosen, was assigned to the new head segment. (Note that g is still the root-mean-square value of the segment free energy, as before.) The total free energy of the chain, G, was the sum of these g-values over all segments. The δx created in this way were approximately $N^{1/2}$ times smaller than those used before, and the computations were corresponding slower.

The results with these short steps are qualitatively similar to those with the long steps, with some modest quantitative differences. As an example we present Figure 6 to compare with Figure 2; the same parameters, except for the step length, were used in each. The minima are shallower with the short steps of Figure 6, but otherwise the effects are much the same.

Low Fields. Free-energy trapping involves competition between three quantities: the free energy, G, which creates

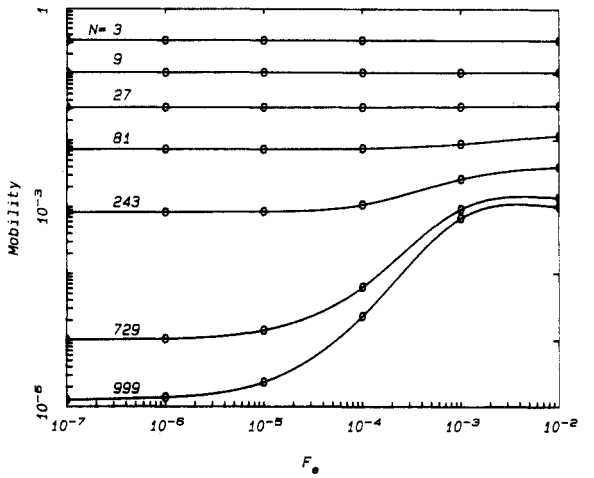

Figure 7. log–log plot of mobility against field for probes of various sizes; a = 0 and g = 0.1.

traps, the field F_e, and the concentration gradient dW/dx; the latter two quantities pull the probes out of the traps. Traps can occur with long chains even when g is very small if the field is weak enough. For example, we show Figure 7, where g is only one-tenth of k_bT. Instead of plotting as in Figures 1–4, we have emphasized the field effect by using the field on a log scale as the abscissa. We see that the mobility, starting at the reptation value at high fields, sinks to a field-independent plateau at low fields. At the right of Figure 7 the field dominates, and simple reptation theory gives the correct mobility; at the left trapping dominates for the larger values of N, and the mobility is strongly reduced. Also at the left the histogram of mobilities narrows to a satisfactory value (data not shown).

5. Results: Diffusion

This plateau at low field allows us to compute the effect of trapping on the diffusion constant. The migration velocity, $\langle \dot{x} \rangle$, can be thought of as the ratio of the driving force, NqE, to a resistance coefficient, ρ. While this ρ is generally a function of the field, its low-field limit is related to the x-coordinate diffusion constant. (We ignore modest effects due to the counterion motion in electrophoresis.) In getting the relative mobility, $\langle \dot{x} \rangle / \langle \dot{x}_0 \rangle$, eq 21, we have divided out qE. The relative mobility is therefore proportional to N/ρ. By Einstein's relation, the x-coordinate diffusion constant, D_x, is k_bT/ρ; therefore, D_x is proportional to the value of our relative-mobility low-field plateau divided by N. The proportionality constant is k_bT/ζ, to which it has not been necessary to assign a numerical value up to now. Since ζ, the resistance coefficient in s-space of one segment, is independent of N, we can define a constant, $K = k_bT/\zeta$. Thus, we get D_x, except for the undetermined constant factor K, as

$$D_x = \frac{K}{N} \lim_{F_e \to 0} \frac{\langle \dot{x} \rangle}{\langle \dot{x}_0 \rangle} \tag{34}$$

with $\langle \dot{x} \rangle / \langle \dot{x}_0 \rangle$ to be taken from the low-field limit of plots like Figure 7.

Effect of Traps. We plot this diffusion constant (with K = 1 for illustration) against N in Figure 8 for three values of g: 0, 0.1, and 0.5. While the g = 0 plot gives the usual reptation[3,4] slope of −2, the other two plots decline much more steeply at large N; this is the result of trapping.

The effect of the depth of a trap on the rate of migration through the trap can be found from a simple calculation along lines suggested by Ferrari, Goldstein, and Lebowitz.[27] We multiply eq 17 by the integrating factor e^{Ψ} with Ψ =

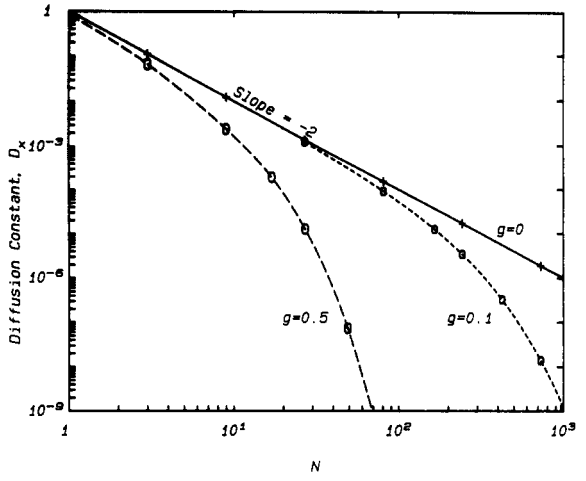

Figure 8. log–log plots of the diffusion constant, D_x, calculated from the low-field limit of plots like those in Figure 7, $a = 0$, as a function of N.

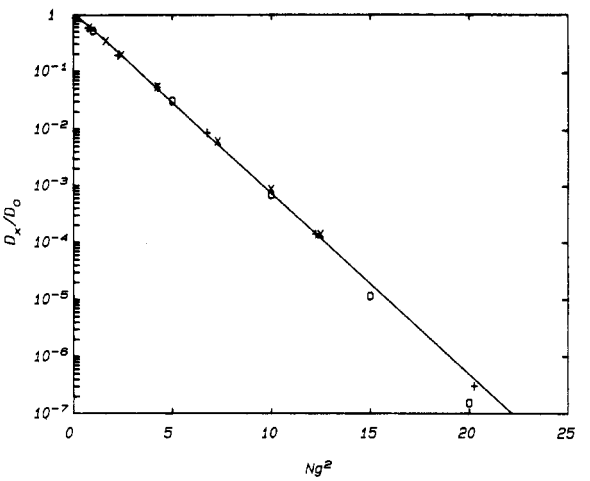

Figure 9. Semilog plots of the ratio of the diffusion constant, D_x, to the pure-reptation diffusion constant, D_0, as a function of Ng^2. Data of Figure 8 and theory from eq 39. O, theory. Data: ×, $g = 0.1$; +, $g = 0.5$.

$(NF_e + G)/k_bT$ and integrate from 0 to x where, as before, x is large and negative. The field F_e is assumed to be positive and finite. After rearranging and dropping a negligible term containing the exponential of xF_e, we get

$$W = -e^{NF_e x}e^{-G(x)}\int_0^x \frac{e^{-NF_e x'}e^{G(x')}}{P(x')}\,dx' \tag{35}$$

We now average over an ensemble of paths through the gel, recognizing that $G(x)$ is not correlated with $G(x')$ as long as $x - x' > L$ and that neither is correlated with $P(x)$ in our model; the averages of these three quantities can thus be done independently of each other. Since the averages are independent of x', we can factor them out, do the integration, and get

$$W = \langle e^{-G}\rangle\langle e^{G}\rangle\langle 1/P\rangle/NF_e \tag{36}$$

By eq 21 the mobility then becomes

$$\frac{\langle \dot{x}\rangle}{\langle \dot{x}_0\rangle} = (\langle e^{-G}\rangle\langle e^{G}\rangle\langle 1/P\rangle)^{-1} \tag{37}$$

By eq 34 D is proportional to the limit of this divided by N as F_e approaches 0. We have already seen that when g, and hence G, is zero, we get the usual reptation result; this arises from the $\langle 1/P\rangle$ factor. Calling the reptation value D_0, we thus have

$$D_x/D_0 = (\langle e^{-G}\rangle\langle e^{G}\rangle)^{-1} \tag{38}$$

In the two factors on the right-hand side the mean value of G cancels out, so D_x/D_0 depends on the fluctuation in G. We are thus led to suggest that the diffusion constant might deviate significantly from D_0 when Ng^2 is greater than unity. For the data of Figure 8 this would occur at $N = 4$ for the $g = 0.5$ curve and at $N = 100$ for the $g = 0.1$ curve, and in fact this appears to be true.

Exponential Dependence on *N*. It is possible to evaluate the averages over G in the limit of small F_e where the frequency of occurrence of G along x is given only by eq 31. The result is

$$\frac{D_x}{D_0} = \frac{2e^{Ng^2/2}}{Ng^2}\left(\int_0^{N^{1/2}g/2} e^{y^2}\,dy\right) \tag{39}$$

where the integral, called Dawson's integral, is available in tables.[28] Successive integration by parts leads to an asymptotic series

$$\frac{D_x}{D_0} = \frac{(Ng^2)^2e^{-Ng^2}}{4}\left(1 - \frac{4}{Ng^2} + \ldots\right) \tag{40}$$

Thus in the limit of large N the dependence of D_x/D_0 on N is exponential. Numerical values from the tables are plotted on a log scale in Figure 9 together with our calculated numbers from Figure 8, and it is seen that a straight line gives a good fit. The slope of the line is only 0.732 instead of unity as eq 40 would suggest; this is the effect of the front factor. Since D_0 scales as N^{-2}, D_x itself should have at large N a dependence on N that is close to pure exponential.

6. Discussion

We have found that even weak interactions between the probe chain and the gel can complicate the simple reptation picture and can have dramatic effects on both the diffusion constant and electrophoretic mobility. (We recall again that we are considering only the tight reptation model where the probe segments are longer than the pores of the matrix.) Random fluctuations in the strength of the interactions along the probe as it moves lead occasionally to locations of low free energy which can act as traps and from which the probe only slowly escapes. In the case of diffusion the phenomenon is added to the usual random walk, and its effect is to reduce the value of the diffusion constant below the simple reptation value, the reduction becoming larger with longer probes and converting the dependence on N from power law to exponential. (A reduction below the reptation value was also found by Muthukumar and Baumgärtner[12,13] in their model with entropic barriers.) This behavior is in accord with the common experimental observation that the diffusion constant of chains of large N in matrices falls faster with N than the reptation model predicts.[7-11] This was true when the matrix was a porous glass as found by Guo et al.,[10] a gel as found by Rotstein and Lodge,[1] or even un-cross-linked but entangled linear chains (Kim et al.[8] and Nemoto et al.[9]).

As examples of significant interactions, we can first suggest entropy reductions of the kind considered by Muthukumar and Baumgärtner.[12,13] To change the g of a segment by $0.5k_bT$, corresponding to the extreme curves of Figures 2–4, it would be necessary to reduce the volume of configuration space available to the segment by a factor of only $\exp(1/2) = 0.607$, where we have used Boltzman's

formula for the entropy. A volume-reduction factor of this size should occur frequently in a random matrix. As another example, consider a chain segment to be one "Kuhn length" (equal to two persistence lengths); forcing it to bend into a 1-rad circular arc to fit into a particular space in a gel would cost k_bT of energy, enough to produce obvious trapping in a chain of many segments.

The effect of trapping is more complex in the case of electrophoretic mobility, where the strength of the field is also important. Here the effect of trapping is strongest at intermediate probe sizes. This comes about because of the different probe-size dependences of the contributions of the interaction free energy, G, and field, F_e, to the total force, eq 32. We have already noted that the root-mean-square fluctuations in G that create traps increase as the square root of probe length N. On the other hand, the field contribution increases with the first power of the probe length. For short probes the values of G are too small to make effective traps, while for very long probes the field contribution to the force overwhelms the contribution of G; it is only at intermediate lengths that G is important. The net result is a depression of the mobility at intermediate probe lengths, the depth of the depression depending on the relative sizes of g and F_e. The slope of the dependence of mobility on size is steepened on the low side of the depression and flattened, or even reversed, on the high side, as in Figures 2–4.

This initial steepening could explain some of the high slopes seen by Calladine et al.[5] and by Arvanitidou and Hoagland.[6] The flattening at higher probe lengths is very well-known and has hitherto been attributed to orientation,[16] as shown for example by the higher curves in Figure 3. We suggest that free-energy trapping may also contribute to it. In Figure 2, where orientation has been completely turned off, note that the middle curves still flatten at intermediate N.

Free-energy trapping may also be partially the cause of "band inversion" in gel electrophoresis, where the mobility of intermediate-sized probes is less than that of both smaller and larger ones, an effect that is sometimes found at higher gel concentrations.[20-24] This is just the effect seen in the lower curves of Figures 2 and 3. This effect is usually attributed to geometric trapping. We propose that free-energy trapping may also be a contributing cause, if g becomes larger at higher gel concentrations where the contacts between the probe and the gel involve more elastic energy. (On the other hand, the gel probably becomes less heterogeneous at higher concentrations, so, lacking a theory for the dependence of g on gel structure, it is not clear what the total effect on g may be.)

We are concerned in this paper with the general effects of free-energy trapping, not with any detailed molecular mechanism. To illustrate the point, we have employed a simple model most applicable to short chains in a tight gel at low fields. Also we are not dealing with physical blind-alley traps or other kinds of traps that permanently absorb the probe,[25] important though these may be. (The molecular mechanism of one example of free-energy trapping has been examined in work by Levene,[26] where the reduction of the gel-electrophoretic mobility by intrinsic bends in DNA was calculated.) In effect, we are asserting that any energetic or entropic interaction between the probe and the matrix will produce the effects discussed here, as long as the interaction depends on the position of the probe but not explicitly on time and as long as the interaction fluctuates as a random function of the position of the probe. The low points of the free energy are traps and the high points barriers; of the two, the traps have greater effects on the motion of the probe because they are places in which the probe stays a long time.

The requirement that the interaction free energy be a function of position but not of time limits us to situations in which the matrix changes conformation much more slowly than the probe or does not move at all. In other words, we are limited either to probes in permanently cross-linked gels[11] or porous glasses[10] or to mixtures of polymers in which one component, the probe, is much smaller than the other, the matrix.[8,9] If the matrix moves too fast, the traps will be evanescent and will have little effect on the motion of the probe.

7. Conclusion

We propose that the addition of a randomly fluctuating free energy of interaction between segments of the probe and the surrounding matrix helps to explain observations of strong dependences of the diffusion constant and electrophoretic mobility on chain length that simple reptation theory does not explain. We have attempted to illustrate the point in this paper by the addition of a randomly fluctuating free energy to the simple tight-tube reptation model (with random-flight tubes, but without tube renewal). Even though this model is highly simplified, we suggest that trapping effects are a more general effect and are likely to appear even in more refined models.

Acknowledgment. We are indebted to Wesley Ames for suggestions concerning the manuscript. This work has been supported by NIH Grant GM11916.

References and Notes

(1) Lerman, L. S.; Frisch, H. L. *Biopolymers* **1982**, *21*, 995.
(2) Lumpkin, O. J.; Zimm, B. H. *Biopolymers* **1982**, *21*, 2315.
(3) de Gennes, P.-G. *Scaling Concepts in Polymers Physics*; Cornell University Press: Ithaca, NY, 1979; p 227.
(4) Doi, M.; Edwards, S. F. *The Theory of Polymer Dynamics*; Oxford University Press: Oxford, U.K., 1986; pp 205–6.
(5) Calladine, C. R.; Collis, C. M.; Drew, H. R.; Mott, M. R. *J. Mol. Biol.* **1991**, *221*, 981.
(6) Arvanitidou, E.; Hoagland, D. *Phys. Rev. Lett.* **1991**, *67*, 1464.
(7) Phillies, G. D. J. *Macromolecules* **1986**, *19*, 2367.
(8) Kim, H.; Chang, T.; Yohanan, J. M.; Wang, L.; Yu, H. *Macromolecules* **1986**, *19*, 2737.
(9) Nemoto, N.; Kishine, M.; Inoue, T.; Osaki, K. *Macromolecules* **1990**, *23*, 659.
(10) Guo, Y.; Langley, K. H.; Karasz, F. E. *Macromolecules* **1990**, *23*, 2022.
(11) Rotstein, N. A.; Lodge, T. P. *Macromolecules* **1992**, *25*, 1316.
(12) Baumgärtner, A.; Muthukumar, M. *J. Chem. Phys.* **1987**, *87*, 3082.
(13) Muthukumar, M.; Baumgärtner, A. *Macromolecules* **1989**, *22*, 1937, 1941.
(14) Honeycutt, J. D.; Thirumalai, D. *J. Chem. Phys.* **1990**, *93*, 6851.
(15) Lumpkin, O. J.; Levene, S. D.; Zimm, B. H. *Phys. Rev. A* **1989**, *39*, 6557.
(16) Lumpkin, O. J.; Déjardin, P.; Zimm, B. H. *Biopolymers* **1985**, *24*, 1573.
(17) Slater, G. W.; Noolandi, J. *Biopolymers* **1986**, *25*, 431.
(18) Déjardin, P. *Phys. Rev. A* **1989**, *40*, 4752.
(19) Zimm, B. H. *J. Chem. Phys.* **1991**, *94*, 2187.
(20) Noolandi, J.; Rousseau, J.; Slater, G. W.; Turmel, C.; Lalande, M. *Phys. Rev. Lett.* **1987**, *58*, 2428.
(21) Slater, G. W.; Rousseau, J.; Noolandi, J. *Biopolymers* **1987**, *26*, 863.
(22) Doi, M.; Kobayashi, T.; Makino, Y.; Ogawa, M.; Slater, G. W.; Noolandi, J. *Phys. Rev. Lett.* **1988**, *61*, 1893.
(23) Slater, G. W.; Turmel, C.; Lalande, M.; Noolandi, J. *Biopolymers* **1989**, *28*, 1793.
(24) Bell, L.; Byers, B. *Anal. Biochem.* **1983**, *130*, 527.
(25) Models of diffusion with traps that permanently absorb the diffusing object have been widely discussed; for review; see: Weiss, G. H. *J. Stat. Phys.* **1986**, *42*, 3.
(26) Levene, S. D.; Zimm, B. H. *Science* **1989**, *245*, 396.
(27) Ferrari, A.; Goldstein, S.; Lebowitz, J. L. In *Statistical Physics and Dynamical Systems*; Fritz, J., Jaffe, A., Szasz, D., Eds.; Birkhauser: Boston, MA, 1985; pp 405–441. See also: Golden, K.; Goldstein, S.; Lebowitz, J. L. *Phys. Rev. Lett.* **1985**, *55*, 2629.
(28) Abramowitz, M.; Stegun, I. *Handbook of Mathematical Functions*; Dover: New York, 1965.